

EVOLUTION OF STRUCTURE IN NUCLEI:
MEDITATION BY SUB-SHELL MODIFICATIONS
AND RELATION TO BINDING ENERGIES*

R.F. CASTEN

Wright Nuclear Structure Laboratory, Yale University
272 Whitney Avenue, New Haven, Connecticut, USA
and

Institut für Kernphysik, Universität zu Köln, 50937, Köln, Germany

R.B. ÇAKIRLI

Istanbul University, Department of Physics, Istanbul, Turkey

(Received October 3, 2008)

Understanding the development of configuration mixing, coherence, collectivity, and deformation in nuclei is one of the crucial challenges in nuclear structure physics, and one which has become all the more important with the advent of next generation facilities for the study of exotic nuclei. We will discuss recent work on phase/shape transitional behavior in nuclei, and the role of changes in sub-shell structure in mediating such transitional regions. We will also discuss a newly found, much deeper, link between nuclear structure and nuclear binding energies.

PACS numbers: 21.10.Re, 21.60.Cs, 21.60.Ev

1. Introduction

One of the great challenges of modern nuclear structure physics is understanding the evolution of structure, in particular, the development of collectivity, phase transitional behavior, and deformation — both phenomenologically and in terms of the underlying microscopy. This effort has expanded tremendously in recent years with the advent of new generations of facilities for the production and study of exotic nuclei, and of instruments (ranging from separators and spectrometers to select nuclei of interest, to advanced gamma ray detectors to study decay transitions, to trapping and storage ring techniques for mass measurements).

* Presented at the Zakopane Conference on Nuclear Physics, September 1–7, 2008, Zakopane, Poland.

In this work we tackle two issues, the nature of shape-changing regions, especially the role of changes in sub-shell structure, and the effects of collectivity and configuration mixing on nuclear binding energies. In the latter, we will show a deeper and far more sensitive relation between masses and collectivity than has heretofore been exploited. This work is based largely on Refs. [1,2] and has been strongly influenced by the earlier work of Refs. [3–9].

2. Shape transitional regions and changes in sub-shell structure

Nuclei very near closed shells can be described in terms of simple shell model configurations. As both valence protons and neutrons are added, configuration mixing develops (we will see another aspect of this in the next section), collectivity emerges, and nuclei evolve to well deformed shapes. Since this process is dominated by interactions among the valence nucleons, it is not surprising that it can develop rather quickly with N and Z : a given change in N or Z represents a far larger change in valence nucleon number. However, the rapidity of nuclear shape transitions remains startling and more rapid than the simple counting above would indicate. This is shown in Fig. 1 which shows changes in $R_{4/2} = E(4_1^+)/E(2_1^+)$ (called $\Delta R_{4/2}(Z, N)$). Regions of rapid change are highlighted. One sees that, in several mass

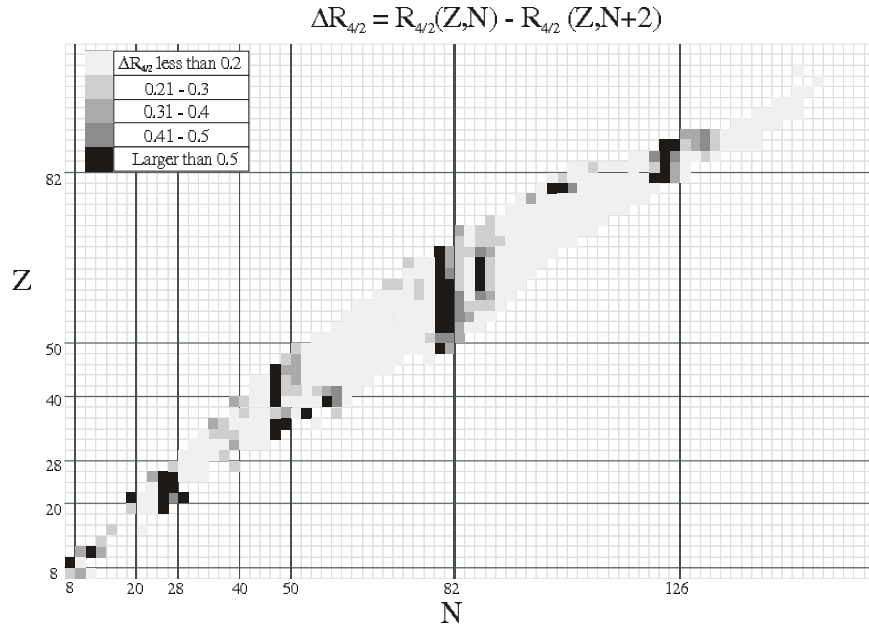


Fig. 1. Plot of $|\Delta R_{4/2}|$ across the nuclear chart, highlighting especially the regions, slightly beyond shell closures, where $R_{4/2}$ changes very rapidly.

regions, a few proton and neutron numbers distant from magic numbers, there are extremely rapid changes, leading from $R_{4/2}$ values typical of near vibrational nuclei, ~ 2.3 , to values characteristic of developing rotational spectra with $R_{4/2} > 3.0$, within a space of just two neutrons.

These results suggest that other mechanisms are at work beyond the simple addition of a couple of nucleons with their interactions. It is well known [3–5, 8] that changes in sub-shells are a key ingredient. It is the purpose of this section to discuss a simple approach to identifying cases where changes in sub-shell structure strongly mediate the development of collectivity and deformation. We will show a technique that reveals such changes by inspection, that identifies the nucleon type which experiences the sub-shell change, and identifies the sub-shell at issue. This is, moreover, a method that relies on only the simplest data, and therefore should be useful in new regions of nuclei far from stability.

The idea is illustrated in Fig. 2 which shows $R_{4/2}$ values for the well-studied $A \sim 150$ region. The figure demonstrates both the point just referred to (see below) but also highlights more generally the value of looking at the same data from different perspectives. The left panel shows $R_{4/2}$ against neutron number for several Z values. One sees, overall, a clear onset of deformation as $R_{4/2}$ increases with N from ~ 2 to ~ 3.33 . It is hard to easily see much more than this at a quick glance. Closer inspection, though, does show a “crossing” pattern where $R_{4/2}$ values for ${}_{60}\text{Nd}$ to ${}_{66}\text{Dy}$ rise from below (for $N < 90$) to above (for $N > 90$) those for ${}_{56}\text{Ba}$ and ${}_{54}\text{Xe}$.

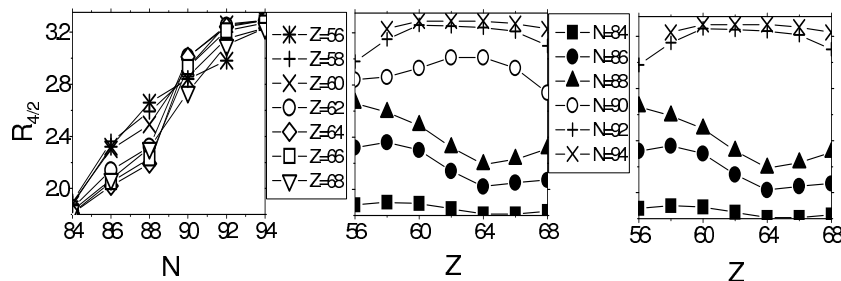


Fig. 2. $R_{4/2}$ values for the rare-earth region plotted against neutron number on the left, and against proton number in the middle and right panels. The right panel is identical to the middle panel except for the removal of the transitional $N = 90$ nuclei in order to highlight the bubble pattern without these intermediate nuclei. Figure based on Ref. [1].

In the middle panel we show exactly the same data, but now plotted against Z for several isotonic sequences. The results are, simply put, dramatic. A clear, and sudden, change from concave to convex curves occurs across $N = 90$. This forms a “bubble” pattern. The concave curves show

$R_{4/2}$ values around 2.4 or less. These are typical of spherical nuclei with anharmonic vibrational excitation modes. The convex curves lie at or above $R_{4/2} \sim 2.8$ and peak near $R_{4/2} \sim 3.33$, typical of well-deformed nuclei. Note the key point that the difference in these curves is greatest near $Z = 64$ where the respective curves show minima and maxima. It is well known that $R_{4/2}$ is the smallest near magic numbers and maximizes in well-deformed nuclei. Thus, there is no escaping the conclusion that $Z = 64$ acts here as a magic number (albeit without as large a gap as is typical, for example, in the “classic” magic numbers such as 50, 82, and 126) for $N < 90$, and that it disappears (in which case $Z = 64$ is near mid-shell in the $Z = 50$ –82 major shell) for $N > 90$. This is the kind of extraordinarily rapid shape change referred to above. Note that the variable (N or Z) for which a bubble pattern appears is the type of nucleon which experiences the sub-shell change.

None of these structural ideas are new, and the role of sub-shell changes has been thoroughly discussed [3–5, 8]. What is new is the presentation of these pairs of “crossing” and “bubble” plots as a simple and visually compelling technique to spot the mediation of shape transition regions by sub-shell changes in the underlying sequence of single particle levels.

The right panel shows another aspect of shape transitional regions that focuses on the fact that nuclei contain integer numbers of nucleons, and hence structure changes discretely with N and Z . In a region of rapid change, therefore, it can happen that structure “jumps” over the transitional (critical) point, or, in other cases, such as the $A \sim 150$ region, one set of nuclei — those with $N = 90$ — land almost exactly at the critical point. Indeed, it is this which has led to recent descriptions of nuclei in first order phase transitional regions by so-called critical point symmetries [10, 11] such as, $X(5)$, and the realization [12] that nuclei such as ^{152}Sm reflect the predictions of such descriptions.

In the right panel, we have therefore removed the $N = 90$ points to see more clearly the structure of this region devoid of the set of transitional isotones. The bubble appears even more clearly.

These results, therefore, provide a simple and virtually immediate method to identify sub-shell mediation of transitional regions. Of course, the underlying mechanism is that the disappearance of a sub-shell immediately increases the effective number of valence nucleons and their interactions [3–5].

While $R_{4/2}$ is a relatively easy-to-measure observable, at the extremes of nuclear accessibility, often one only observes the mass, lifetime, and the first excited state. Therefore, it is fortunate that $E(2_1^+)$ provides an equally useful indicator. Since $E(2_1^+)$ decreases as deformation sets in, oppositely to the growth of $R_{4/2}$, it is more useful to use $1/E(2_1^+)$ instead. This is shown in Fig. 3. We show the $A \sim 150$ region on the top for easy comparison with

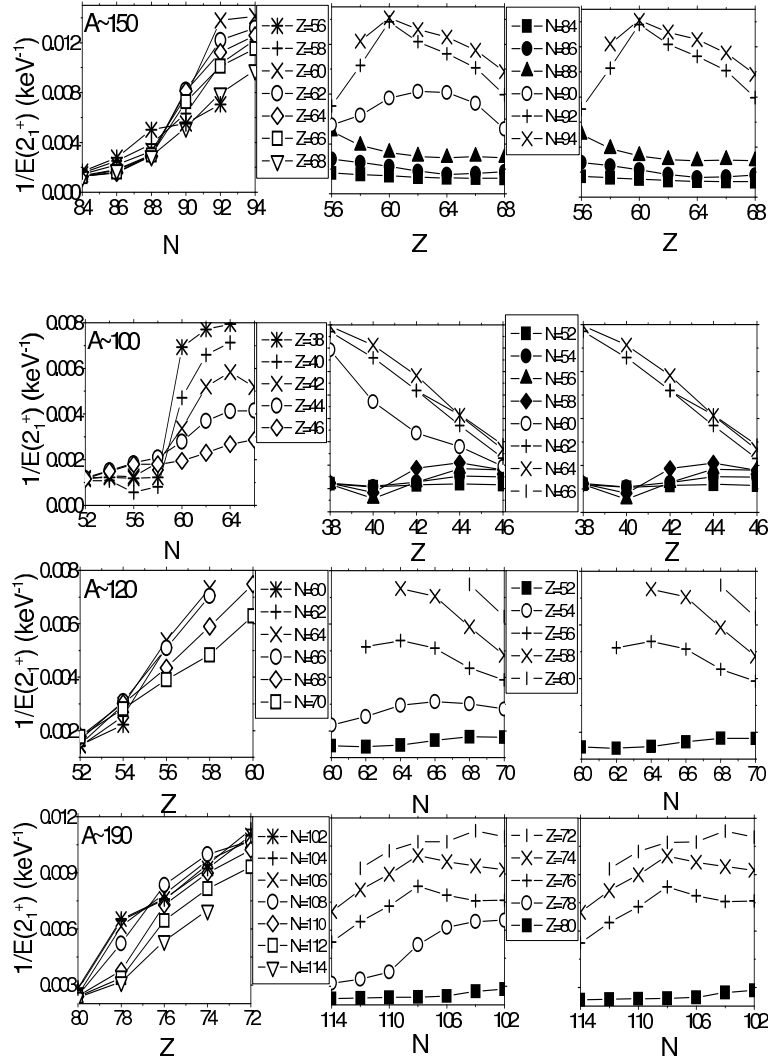


Fig. 3. Similar to Fig. 2, except for $1/E(2_1^+)$, and for four different mass regions. Figure based on Ref. [1].

Fig. 2. The same analysis and conclusions result as for $R_{4/2}$ except that these data are easier to obtain. Fig. 3 shows three other regions as well: $A \sim 100$, 120, and 190. The data for $A \sim 100$ and 150 show the well-known changes in proton shell gaps at $Z = 40$ and 64. The $A \sim 120$ and 190 regions are somewhat muted but still show clear crossing and bubble patterns. However, note that they are now in the neutron sector, at $N \sim 64$ and ~ 108 . We see again then that the nucleon type whose plot shows a bubble pattern is the type that experiences the sub-shell change.

3. Binding energies and structure

The development of advanced Penning traps and storage rings to measure nuclear masses is one of the most important experimental developments in the study of nuclear physics [13]. Too frequently in the past the communities involved in mass measurements and those pursuing nuclear structure studies *per se*, have had somewhat of a disconnect. Phrased alternately, with a few exceptions, direct links between masses and structure has not been a prime focus. Of course, masses are of great interest globally in defining very general mass formulas. They are also of interest locally through a variety of focused mass formulas that link nearby nuclei and test for such aspects of structure as isospin. Two dramatic and direct links of masses and structure are evident in Fig. 4 which shows two-neutron separation energies, S_{2n} , against neutron number for a portion of the nuclear chart. There are three very obvious features, the sudden drop after magic numbers reflecting the lower binding of the next major shell, the local increase near $Z = 62$ and $N = 90$, reflecting the discontinuity associated with a first order phase transition, which leads to increased binding relative to the general systematics, and, of most interest to us here, the sequences of nearly parallel, nearly linear, S_{2n} values for successive chains of isotopes. Indeed, these latter are often approximated by a functional form $A + BN$. However, closer inspection shows that there are deviations in linearity, as seen, for example, in the Er isotopes. The linear behavior itself can be derived [14] from the leading terms in the Weizsäcker mass relation [15]. The deviations from linearity point to different physics not included in that approach, specifically extra binding from configuration

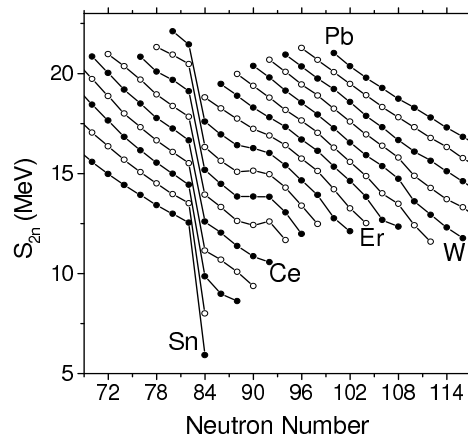


Fig. 4. Two neutron separation energies for a region of heavy nuclei showing the effects of shell closures, of quantum phase transitions, and curvatures reflecting contributions to binding from collective effects.

mixing and collectivity that depresses the ground state. There is no *a priori* reason that such effects should be linear, as indeed, is shown by the bulge (almost a bubble) at $N \sim 90$ in Fig. 4.

It is our purpose here to indicate one surprising result in calculations of the collective component of the S_{2n} values. That is, we write

$$S_{2n}(Z, N) = S_{2n}^0 + S_{2n}(\text{collective}), \quad (1)$$

where $S_{2n}(\text{collective})$ is the part of $S_{2n}(Z, N)$ that comes from the binding associated with the correlations in the collective Hamiltonian, and S_{2n}^0 is the remainder.

The collective component can be calculated with any appropriate collective model. We will use the IBA [16] because of its historic success, its parameter efficiency and the broad range of collective structures it encompasses. $S_{2n}(\text{collective})$ in the IBA is simply given by the differences in binding energies of two successive even-even isotopes. We use the simple Hamiltonian [17–19]

$$H = c \left[(1 - \zeta) \hat{n}_d + \frac{\zeta}{4N_B} Q \cdot Q \right], \quad (2)$$

where $Q = s^\dagger \tilde{d} + d^\dagger s + \chi (d^\dagger \tilde{d})$ and N_B is the boson number.

The structure of any given nucleus is given solely by ζ and χ , where ζ controls the competition between spherical and deformed structure and χ controls the axiality. ζ varies from zero (spherical vibrator or U(5) limit) to unity (for deformed nuclei, in which case $\chi = -\sqrt{7}/2 = -1.32$ gives the SU(3) symmetry and $\chi = 0$ gives O(6)). Having chosen ζ and χ to fit the relative excitation spectra and transition rates of a nucleus, the absolute energy scale is fixed by normalizing the scale parameter c .

Numerous nuclei have been studied with this Hamiltonian, especially in the rare earth region [6]. We will therefore not do any re-fitting but rather use existing parameters selected to fit the level schemes and look at their predictions for binding energies and S_{2n} values. We choose the Er isotopes to exemplify this. (We note that they are not “typical” but do show one of the most dramatic examples of the point we will make.) In Ref. [6] it was pointed out that, in Er with $N = 100$, there are two excited 0^+ states, at $E = 1217$ and 1422 keV, and that it is not *a priori* clear which one is the collective one. (Of course, they could be mixed but that is not the issue here). Therefore, two fits were done in Ref. [6], each of which fits one of these two states. We used both sets of parameters here.

Our results are shown in Fig. 5, which gives the collective (IBA) contribution to the binding energy. The results are startling. The trend is smooth until $N = 100$ where it forks, giving different values for the two sets of parameters. (The parameter values are $\zeta = 0.82$, $\chi = -0.36$ and $\zeta = 0.96$,

$\chi = -0.25$, with the factor c in Eq. 2 scaled to reproduce the actual 2_1^+ energy. Note that ζ and χ are very close to each other, relative to their full allowed ranges of 0 to 1 and -1.32 to 0, respectively). The key point we make here is that, for $N = 100$, the difference between the two binding energies is huge, over 4 MeV.

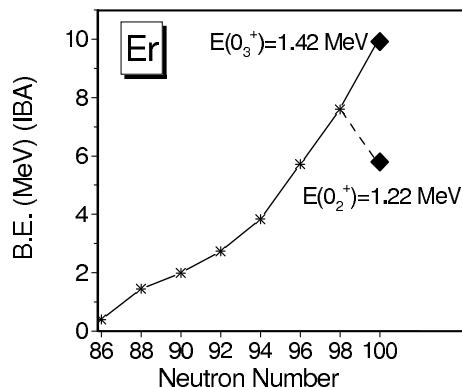


Fig. 5. Collective contributions to binding energies calculated for the Er isotopes in the IBA (see text). Figure based on Ref. [2].

This result was totally unexpected: how can the process of fitting two 0^+ states, differing in energy by only 200 keV, give ground state binding energies differing by 4 MeV? We note in passing that this is not due to mixing of the ground and excited 0^+ states (the required mixing matrix elements would have to be ~ 10 MeV). Rather, it is due to the fact that different parameter sets in the IBA space lead to different degrees of collective binding, which, for some reason, not yet fully understood, is highly magnified. We have investigated other cases and, while this is the largest effect we have found, many other cases lead to differences in S_{2n} values of 1–2 MeV. The effect is largest near mid-shell for highly deformed nuclei.

Such differences in binding lead to corresponding differences in S_{2n} values far beyond the deviations from linearity seen in Fig. 4, including even the phase transitional region. Clearly, Fig. 5 allows one, virtually by inspection, to select which 0^+ state gives predictions consistent with the data. It should be clear from the smooth S_{2n} systematics for Er in Fig. 4 and the large effects in Fig. 5, that only the 1.42 MeV 0^+ state gives consistent results.

The implications of this are hard to overestimate. These results show a very strong link between masses and structure, that is, a dependence of binding energies on structure in well-deformed nuclei that is far larger than heretofore recognized. We note that Ref. [9] found a similar effect but for transitional nuclei in which the two sets of IBA parameters differed very significantly (they spanned half the symmetry triangle). Comparison of cal-

culated and experimental binding energies even allowed us to suggest which excited 0^+ state between 1200 and 1500 keV in Er with $N = 100$ is the collective one. Such an extreme sensitivity has not heretofore been recognized or exploited and provides a new tool to understand collective structure in nuclei based, again, on the simplest-to-obtain data. This suggests that one should not henceforth carry out structure calculations without also asking if such calculations reproduce the binding energy data. Conversely, subsequent mass measurements should always seek to determine possible effects of the associated binding energies on understanding the structure and the excitation spectrum.

4. Summary

We have investigated two aspects of collectivity and structural evolution. We showed a simple technique, based on easy-to-obtain data, even in nuclei far from stability, that allows one to determine when shape transition regions are mediated by underlying sub-shell changes, and to identify which sub-shell dissolution is at work. Secondly, we studied the collective component of nuclear binding energies and found, using the IBA model, a highly magnified sensitivity to structure such that, for example, calculations of binding energies can, in some cases, even help distinguish the nature of particular excited states and help decide subtle aspects of the structure of particular nuclei.

We would like to thank a number of people for very helpful discussions and contributions that have greatly benefited this work: Mark Caprio, Ryan Winkler, Magdalena Kowalska, Klaus Blaum, D.S. Brenner, Paddy Regan, Victor Zamfir, E.A. McCutchan, Dennis Bonatsos, Francesco Iachello, Witek Nazarewicz, Mario Stoitsov, and Georges Bertsch. Special thanks are due to Mark Caprio for correcting an error in the IBA code. Work supported by the US DOE under Grant No. DE-FG02-91ER-40609 and by the DFG through a Mercator Guest Professorship at the University of Köln, under Grant No. Ko 142/112-1.

REFERENCES

- [1] R.B. Cakirli, R.F. Casten, *Phys. Rev.* **C78**, 041301(R) (2008).
- [2] R.B. Cakirli, R.F. Casten, *Phys. Rev. Lett.* (2009) (in press).
- [3] P. Federman, S. Pittel, *Phys. Lett.* **B77**, 29 (1978).
- [4] P. Federman, S. Pittel, R. Campos, *Phys. Lett.* **B82**, 9 (1979).
- [5] R.F. Casten, D.D. Warner, D.S. Brenner, R.L. Gill, *Phys. Rev. Lett.* **47**, 1433 (1981).

- [6] E.A. McCutchan, N.V. Zamfir, R.F. Casten, *Phys. Rev.* **C69**, 064306 (2004).
- [7] M. Stoitsov, R.B. Çakirli, R.F. Casten, W. Nazarewicz, W. Satula, *Phys. Rev. Lett.* **98**, 132502 (2007).
- [8] K. Heyde, P. Van Isacker, R.F. Casten, J.L. Wood, *Phys. Lett.* **B155**, 303 (1985).
- [9] Garcia Ramos *et al.*, *Nucl. Phys.* **A688**, 735 (2001).
- [10] F. Iachello, *Phys. Rev. Lett.* **87**, 052502 (2001).
- [11] F. Iachello, *Phys. Rev. Lett.* **85**, 3580 (2000).
- [12] R.F. Casten, N.V. Zamfir, *Phys. Rev. Lett.* **87**, 052503 (2001).
- [13] Klaus Blaum, *Phys. Rep.* **425**, 1 (2006).
- [14] R. Fossion, C. De Coster, J. E. Garcia-Ramos, T. Werner, K. Heyde, *Nucl. Phys.* **A697**, 703 (2002).
- [15] C.F. von Weizsächer, *Z. Phys.* **96**, 431 (1935).
- [16] F. Iachello, A. Arima, *The Interacting Boson Model*, Cambridge, England: Cambridge University Press, 1987.
- [17] D.D. Warner, R.F. Casten, *Phys. Rev. Lett.* **48**, 1385 (1982).
- [18] P.O. Lipas, P. Toivonen, D.D. Warner, *Phys. Lett.* **B155**, 295 (1985).
- [19] V. Werner, P. von Brentano, R.F. Casten, J. Jolie, *Phys. Letts.* **B527**, 55 (2002).